Supporting Information

Atmospheric-pressure Plasma-enhanced Spatial ALD of SiO_2 studied by gas-phase Infrared and Optical Emission Spectroscopy

M. A. Mione,[1] V. Vandalon,[1] A. Mameli,[2] W. M. M. Kessels[1,*] and F. Roozeboom[1,2]

[1] Eindhoven University of Technology, Dept. of Applied Physics. PO Box 513, 5600 MB Eindhoven, The Netherlands

[2] TNO-Holst Centre, High Tech Campus 31, 5656 AE Eindhoven, The Netherlands

S1 Derivation of BDEAS flow to reactor chamber from Ar pick-up flow to bubbler

This section explains in more detail how the actual flow of BDEAS to the reactor chamber was calculated knowing the Ar pick-up flow that is fed into the bubbler. The calculated values for the BDEAS flow will be also used in Section S4 for the quantitative analysis of the precursor depletion.

To feed BDEAS to the reactor chamber, a pick-up flow of Ar is dosed by means of a mass flow controller (MFC) and introduced into the BDEAS bubbler which is kept at 20 ± 2 °C. The BDEAS flow exiting the bubbler can be calculated using the so-called 'bubbler equation' [1,2]

$$Q_{precursor} = Q_{pick-up}\frac{p_{precursor}}{p_{pick-up}} = Q_{pick-up}\frac{p_{precursor}}{p_{tot} - p_{precursor}} \quad \text{(S1)}$$

where $Q_{precursor}$ and $Q_{pick\text{-}up}$ are the precursor and the pick-up molar flows, respectively; $p_{precursor}$ and $p_{pick\text{-}up}$ are the partial pressures of precursor and pick-up gas, and p_{tot} is the total system pressure ($p_{tot}=p_{precursor}+p_{pick\text{-}up.}$). This equation is based on the assumption of ideal gas behavior for both gases. When calculating $Q_{precursor}$ we consider that the total flow of Ar and BDEAS to the reactor is kept constant at 1 slm. For each pick-up flow used, in Table S1 we list the BDEAS flows to the reactor chamber in units of slm as well as molecules/min as they were calculated from Equation (S1).

Table S1 Values of the BDEAS flow to the reactor chamber as calculated from the corresponding pick-up Ar flows dosed to the bubbler.

Ar pick-up flow (slm)	**BDEAS flow to the reactor (slm)**	**BDEAS molecular flow (x10^{18} molecules/min)**
0.01 ± 0.01	(1.5 ± 1.0) x 10^{-5}	4.0 ± 0.4
0.05 ± 0.01	(7.5 ± 1.0) x 10^{-5}	2.0 ± 0.4
0.10 ± 0.01	(1.0 ± 0.1) x 10^{-4}	2.6 ± 0.4
0.20 ± 0.01	(3.0 ± 0.1) x 10^{-4}	8.0 ± 0.4

The dosing of the precursor to the reactor is executed consistently for each deposition and therefore the non-systematic errors on the BDEAS flow can be neglected. The uncertainty in the BDEAS flow fed to the reactor will be mainly caused by systematic errors in Equation (S1)

that are due to factors such as the unknown accuracy of the MFC in dosing the Ar pick-up flow, the uncertainty in the vapor pressure of the precursor based on literature values, and the ideal gas assumption that holds for both Ar and BDEAS. To verify the relation between precursor flow and Ar pick-up flow we consider the peak intensity of the Si-H stretching mode at 2100 cm^{-1} in the 'precursor only' infrared spectra and plotted as a function of the corresponding Ar pick-up flow. Figure S1 shows that the intensity of the Si-H peak indeed increases linearly with the Ar pick-up flow. One can expect that for the smallest Ar pick-up flow of 0.01 slm, the corresponding BDEAS flow is also non-zero, which will therefore lead to a non-zero intensity of the Si-H peak. However, this is not the case as the linear fit through the data shows that for the smallest Ar pick-up flow the absorbance of the Si-H peak is zero. This means that, although 0.01 slm of Ar are introduced in the bubbler, the corresponding BDEAS flow exiting the bubbler and fed to the reactor is zero. The intercept of the fit to the x-axis represents the amount of BDEAS that should be picked up by the Ar flow but does not reach the reactor. This might be considered as the typical error in the BDEAS flow.

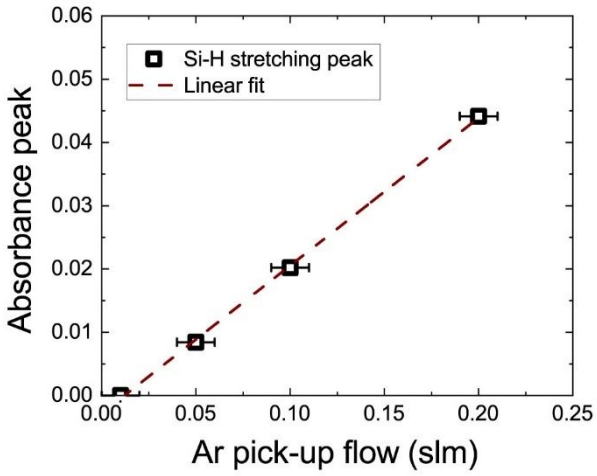

Figure S1 Absorbance peak of the Si-H stretching vibrational mode at 2100 cm^{-1} of the 'precursor only' spectrum plotted as a function of the Ar pick-up flow. The dashed line represents a linear fit through the data.

S2 Distinguishing between byproducts and reactant signal during spectra acquisition

To obtain Figure 4 and Figure 5 of the main manuscript we use two different BDEAS flow settings of 7.5 x 10^{-5} slm and 3.0 x 10^{-4} slm, respectively. This choice was made to enhance the infrared signal of the reaction byproducts with respect to the reactants. Figure S2 shows the region 2600-3100 cm^{-1} of the normalized 'precursor only' and 'precursor-half-cycle' spectra recorded by making use of a high BDEAS flow of 3.0 x 10^{-4} slm and a low BDEAS flow of 7.5 x10^{-5} slm. The 'precursor only' and the 'precursor half-cycle' spectra in Figure 4 share many vibrational modes, yet one extra C-H vibrational mode at 2870 cm^{-1} appears in the 'precursor-half-cycle' spectrum. This mode which is assigned to DEA is less pronounced when using a higher BDEAS flow. In principle, a higher precursor flow leads to more DEA production, but also to more unreacted BDEAS. As a consequence, the signal due to unreacted BDEAS overshadows the infrared signal of DEA. This effect is reduced at lower precursor flows. Hence, a low precursor flow of 7.5 x 10^{-5} slm is preferred to better distinguish the signal of the reaction byproducts from the signal of the precursor.

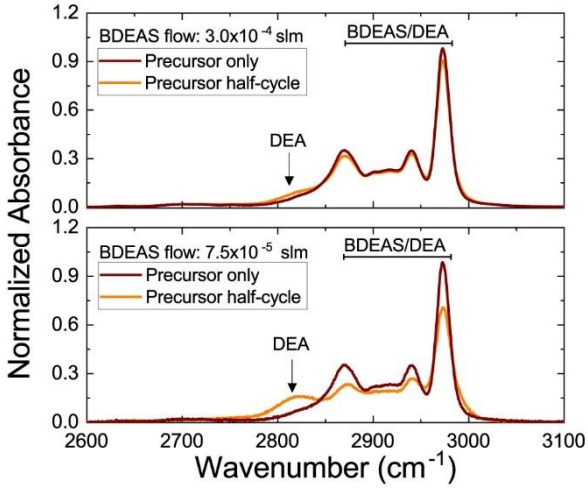

Figure S2 Infrared spectra of the precursor exhaust gas acquired in 'precursor only' mode and in 'precursor half-cycle' mode for two different BDEAS flows.

Figure S3 shows the infrared spectra of the plasma exhaust gas recorded in 'plasma only' mode and in 'plasma half-cycle' mode for the two BDEAS flows mentioned above. When investigating the plasma half-cycle, the extent to which the surface is saturated with adsorbed precursor molecules will determine the intensity of the byproducts signal: the higher the

adsorbed precursor surface coverage, the more byproducts are removed from the surface during the plasma step. Figure S3 shows that a higher precursor flow leads to more byproducts being produced as higher peak intensities for these reaction byproducts are obtained for the higher BDEAS flow. Therefore, to optimize the signal from the byproducts a high BDEAS flow was used during the plasma exhaust analysis. This holds for the infrared spectroscopy investigation as well as for the OES analysis.

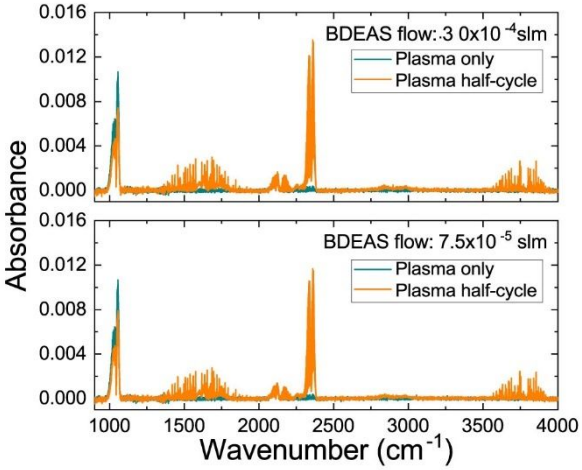

Figure S3 Infrared spectra of the plasma exhaust gas acquired in 'plasma only' mode and in 'plasma half-cycle' mode for two different BDEAS flows.

S3 CO_2 as a reaction byproduct during precursor adsorption

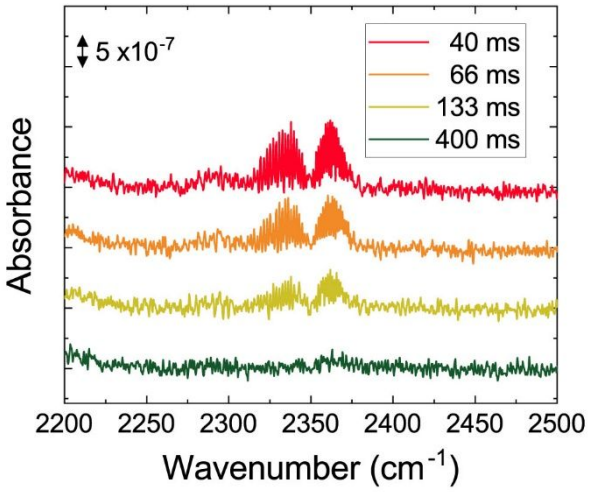

Figure S4 Infrared spectra of the asymmetric stretching mode of CO_2 as measured in 'precursor half-cycle' mode at different exposure times. Data were acquired at 100 °C, a BDEAS flow of 7.5 x 10^{-5} slm and an O_2 flow of 0.08 slm. The CO_2 absorbance decreases with increasing exposure time to the plasma. Spectra have been shifted for clarity.

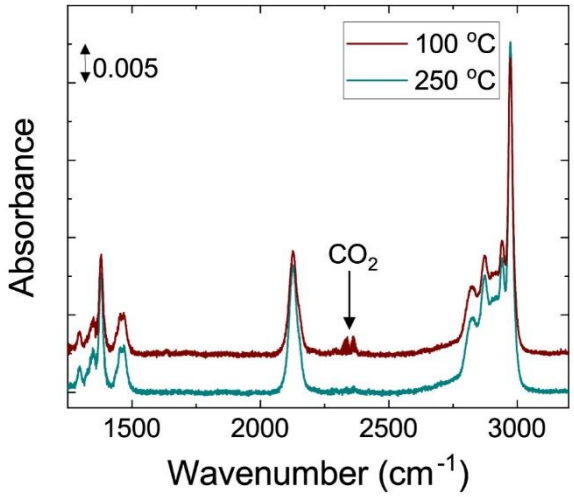

Figure S5 Infrared spectra of the precursor exhaust gas obtained in 'precursor half-cycle' mode at 100 °C and 250 °C. The intensity of the CO_2 peak is higher at 100 °C. The spectra were acquired using an exposure time of 40 ms, a BDEAS flow of 7.5 x 10^{-5} slm and an O_2 flow of 0.08 slm and have been offset vertically for clarity.

S4 Error estimation for the BDEAS depletion and reacted BDEAS flow

The precursor depletion represents the fraction of the BDEAS flow, $Q(BDEAS)_0$, which is depleted by ALD reactions (see Equation (4)). From the precursor depletion and the BDEAS flow, $Q(BDEAS)_0$, the flow of reacted BDEAS can be calculated as

$$Q(BDEAS)_{reacted} = BDEAS\ depletion * Q(BDEAS)_0 = 1 - \frac{A(Si-H)}{A(Si-H)_0} Q(BDEAS)_0 \quad \text{(S2)}$$

To estimate the uncertainties in the integrated peak absorbance values $A(Si\text{-}H)_0$ and $A(Si\text{-}H)$, we considered different baselines for these peaks and determined the spread in the resulting integrated area for equivalent measurements. These uncertainties were negligible compared to the error introduced in the BDEAS flow as described in Section S1. For this reason, we assumed that the error in the reacted BDEAS flow is mainly ruled by the error in the flow $Q(BDEAS)_0$. Table S2 lists the data on BDEAS depletion as plotted in Figure 7 (a) and the data on the reacted flow of BDEAS used in Figure 8.

Table S2 BDEAS depletion and reacted BDEAS flow for two BDEAS flow settings. The estimated errors calculated by making use of the error propagation theory are also given.

Exposure (ms)	$A(Si\text{-}H)_0$	$A(Si\text{-}H)$	**Depletion**	$Q(BDEAS)_0$ **(** x10^{18} **molecules/min)**	$Q(BDEAS)_{reacted}$ **(** x10^{18} **molecules/min)**
40	2.4 ± 0.1	1.2 ± 0.1	0.1 ± 0.1	2.0 ± 0.4	1.0 ± 0.3
66	2.4 ± 0.1	1.4 ± 0.1	0.2 ± 0.1	2.0 ± 0.4	8.3 ± 0.3
133	2.4 ± 0.1	1.8 ± 0.1	0.4 ± 0.1	2.0 ± 0.4	5.3 ± 0.2
400	2.4 ± 0.1	2.1 ± 0.1	0.5 ± 0.2	2.0 ± 0.4	1.7 ± 0.2
40	10 ± 0.1	8.2 ± 0.1	0.20 ± 0.02	8.0 ± 0.4	1.4 ± 0.2
66	10 ± 0.1	8.7 ± 0.1	0.10 ± 0.02	8.0 ± 0.4	1.1 ± 0.2
133	10 ± 0.1	9.2 ± 0.1	0.08 ± 0.01	8.0 ± 0.4	0.6 ± 0.2
400	10 ± 0.1	9.7 ± 0.1	0.03 ± 0.01	8.0 ± 0.4	0.2 ± 0.1

S5 Linking ALD growth with BDEAS depletion

Knowing the precursor depletion is useful to evaluate whether the depleted precursor is consumed for film deposition at the substrate. Potential other reaction pathways may lead to parasitic deposition on reactor walls and delivery lines or to the formation of other gas-phase species from side reaction mechanisms (although rather unlikely for ALD).[3] In order to verify that the depleted precursor is utilized for the deposition of SiO_2 films on the substrate, the BDEAS depletion was plotted as a function of the measured film thickness. Figure S6 shows the results for a BDEAS flow of 3.0 x 10^{-4} slm and indicates that the depletion indeed correlates with the thickness of the SiO_2 films.

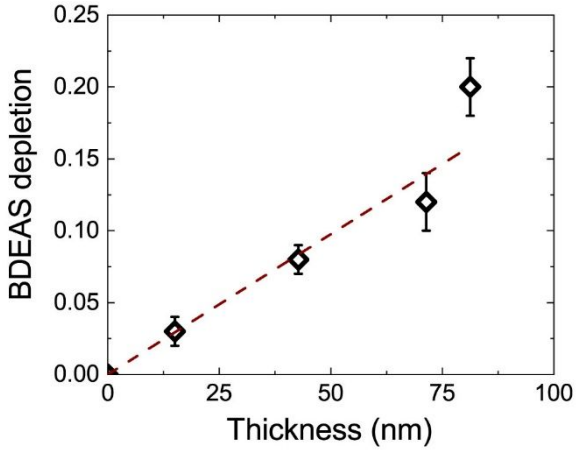

Figure S6 BDEAS depletion as a function of the deposited SiO_2 film thickness. The data were acquired using a BDEAS flow of 3.0 x 10^{-4} slm. The dashed line is a linear fit through the data.

S6 Quantification of the desorbing DEA during the precursor half-cycle

The flow of desorbing DEA was quantified by considering the N-H wagging mode at 727 cm^{-1} in Figure 4. In this case, we used the DEA infrared spectrum in Figure 4 (c) as a reference spectrum. Knowing the flow, $Q(DEA)_0$, used to record this DEA reference spectrum, the desorbing DEA flow is obtained as

$$Q(DEA)_{desorbed} = \frac{A(N-H)}{A(N-H)_0} * Q(DEA)_0 \quad \text{(S3)}$$

Here, $A(N\text{-}H)_0$ is the integrated area of the N-H peak in Figure 4 (c) for the reference flow $Q(DEA)_0$, while $A(N\text{-}H)$ is the integrated area of the N-H peak in the 'precursor half-cycle' spectrum (Figure 4 (a)) which is attributed to the DEA produced during the ALD process.

To estimate the uncertainties in the integrated absorbance values $A(N\text{-}H)_0$ and $A(N\text{-}H)$ in Equation (S3), we considered different baselines for the N-H wagging peaks and determined the spread for equivalent measurements. To estimate the uncertainty in the calibration DEA flow we made the same considerations as for the case of BDEAS in Section S1. Since DEA was fed to the gas cell using an Ar pick-up flow system similar as for BDEAS, the error in $Q(DEA)_0$ can be assumed to be similaras well. Error propagation theory was used to calculate the uncertainties on the desorbed $Q(DEA)_{desorbed}$ /$Q(BDEAS)_{adsorbed}$ flows ratio presented in Figure 8 of the main manuscript.

References

(1) Betsch, R. J. Parametric Analysis of Control Parameters in MOCVD. *J. Cryst. Growth* **1986**, 77 (1–3), 210–218.

(2) Maslar, J. E.; Kimes, W. A.; Sperling, B. A.; Kanjolia, R. K. Characterization of Bubbler Performance for Low-Volatility Liquid Precursor Delivery. J. *Vac. Sci. Technol. A* **2019**, 37 (4), 041506.

(3) Sansonnens, L.; Howling, A. A.; Hollenstein, C. Degree of Dissociation Measured by FTIR Absorption Spectroscopy Applied to VHF Silane Plasmas. *Plasma Sources Sci. Technol.* **1998**, 7 (2), 114–118.